










RESEARCH ARTICLE | NOVEMBER 16 2023

Li–Pd–Rh–D₂O electrochemistry experiments at elevated voltage

Carl Gotzmer; Louis F. DeChiaro  ; Kenneth Conley ; Marc Litz ; Marshall Millett; Jesse Ewing; Lawrence P. Forsley ; Karen J. Long ; William A. Wichart; Pamela A. Mosier-Boss ; John Sullivan ; Efreem Perry, Jr; Oliver M. Barham 



APL Energy 1, 036107 (2023)
<https://doi.org/10.1063/5.0153487>



CrossMark



Applied Physics Reviews

Special Topic: Frontiers in energy materials research: novel measurement, modeling and processing approaches

Submit Today



Li-Pd-Rh-D₂O electrochemistry experiments at elevated voltage

Cite as: APL Energy 1, 036107 (2023); doi: 10.1063/5.0153487

Submitted: 30 April 2023 • Accepted: 1 November 2023 •

Published Online: 16 November 2023



View Online



Export Citation



CrossMark

Carl Gotzmer,¹ Louis F. DeChiaro,^{1,2,a)}  Kenneth Conley,³  Marc Litz,⁴  Marshall Millett,⁵ Jesse Ewing,⁵ Lawrence P. Forsley,⁶  Karen J. Long,²  William A. Wichart,² Pamela A. Mosier-Boss,⁶  John Sullivan,⁷  Efrem Perry, Jr.,¹ and Oliver M. Barham⁸ 

AFFILIATIONS

¹NSWC Indian Head Division, Indian Head, Maryland 20640, USA

²NSWC Dahlgren Division, Dahlgren, Virginia 22448, USA

³Energetics Technology Center, Indian Head, Maryland 20640, USA

⁴Army Research Laboratory, Adelphi, Maryland 20783, USA

⁵U.S. Naval Academy, Annapolis, Maryland 21402, USA

⁶JWK Corporation, Annandale, Virginia 22003, USA

⁷Fibretex Incorporated, Herndon, Virginia 20171, USA

⁸Barham Scientific LLC, Washington, DC 20017, USA

^{a)}Author to whom correspondence should be addressed: louis.f.dechiarojr.civ@us.navy.mil;

Distribution A (23-162): Approved for public release; distribution is unlimited.

ABSTRACT

In 2013, the U.S. Navy disclosed an electrochemistry procedure intended to produce MeV-energy nuclear particles, based on eV-energy electrical inputs, which may be indicative of a new scientific phenomenon. This work is based on the 2013 disclosure and shows initial evidence validating the prior claims of nuclear particle generation. Additionally, several variations on the 2013 electrochemical recipe are made in order to find a highly repeatable recipe for future replications by other teams. The experiments described here produced dense collections of tracks in solid-state nuclear track detectors, radio frequency (RF) emissions, and anomalous heat flux, which are indicative of potential nuclear, or unusual chemical, reactions. Experimental results include tracks in solid-state nuclear track detectors similar in size to tracks produced by 4.7 MeV alpha particles on identical detectors exposed to radioactive Th-230; RF pulses up to 6 dB above the noise floor, which indicate that these signals were likely not background noise and not caused by known chemical reactions; and heat flux of 10 s of kJ, measured to 6 σ significance, over and above input electrical energy, indicative of unknown exothermic reactions. Six out of six nuclear track detectors, utilized in experiments and interrogated for tracks post-experiment, produced positive results that our team attributes to thousands of individual particle impacts in dense clusters, likely with energies between 0.1 and 20 MeV. Similar nuclear particle, thermal, and RF results have separately appeared in prior reports, but in this work, all three categories of anomalous behavior are reported. Results indicate that the 2013 procedure may be a useful guide toward a set of highly repeatable reference experiments, showing initial but not overwhelming evidence of a new scientific phenomenon. Repeatable recipes are shared so that other groups may replicate and extend the present work.

© 2023 Author(s). All article content, except where otherwise noted, is licensed under a Creative Commons Attribution (CC BY) license (<http://creativecommons.org/licenses/by/4.0/>). <https://doi.org/10.1063/5.0153487>

In 1989, electrochemists from the University of Southampton, U.K., and the University of Utah published a study in the Journal of Electroanalytical Chemistry claiming to report nuclear-origin results from experiments based on the metals palladium (Pd) and lithium

(Li) in the heavy water (D₂O)-based electrolyte.¹ The claimed observations of nuclear-origin particles and gamma rays were unexpected due to the use of common laboratory equipment, which was not thought to be able to produce such results. The authors claimed

this as evidence for a new scientific phenomenon: “cold” fusion of deuterium (D, also known as heavy hydrogen) atoms inside the near room temperature experiment. Many of the attempts to replicate these results in the months following the initial announcement were inconclusive and/or not repeatable, and the U.S. Department of Energy recommended against a funding line to continue similar experiments.² The same year, an unrelated study from Brigham Young University, published in *Nature*, also claimed that electrochemistry based on Pd metal in the D₂O-based electrolyte produced nuclear-origin particles³ but received less media attention. Over the next three decades, research efforts in the U.S. Navy,^{4–10} U.S. National Aeronautics and Space Administration (NASA),¹¹ and the internet company Google¹² published work in this area, including some initial positive results. However, no U.S. Government funding line was initiated, despite other countries initiating funding in this area.^{13,14}

In the present effort, a team of scientists and engineers from the U.S. Departments of Defense and Commerce, along with commercial and academic partners, attempted to replicate positive U.S. Navy results disclosed in a 2013 patented electrochemistry procedure.¹⁵ The experimental goal was to look for evidence of nuclear-energy particles, unusual radio frequency (RF), and thermal signatures that would not be expected from chemistry experiments. In addition to the experimental results, modeling was undertaken with

commercially available software, based on quantum mechanical Density Functional Theory (DFT),¹⁶ to determine whether D₂ molecules embedded in Pd lattices could potentially reach vibrational energies in the hundreds of thousands of electron volts, a condition that could lead to D + D fusion within this metallic environment. The project was internally named HIVER (H/Pt/Pd/Rh/Li Versatile-modeling and Evaluation of Results).

Thirty-three numbered experimental runs were completed in total, with varying chemistries and electric/magnetic field orientations. The general procedure consisted of electrolyzing D₂O, with a DC current up to 900 mA passed through 0.25 mm diameter platinum (Pt) electrodes, in the presence of chlorine (Cl) based salts of lithium (Li) palladium (Pd) and Rhodium (Rh) (in some experiments) metals. Pd and Rh metals were reported by other groups to lead to anomalous results, and electrolyzing Li on its own was not, so results from experiments utilizing these chemistries were compared in an attempt to determine whether effects due to Pd and/or Rh could be isolated and better understood. The following main experimental values were monitored across all experiments: temperature inside electrolyte, heat flux through walls of container, RF emissions at the cathode, and nuclear-energy particle damage (tracks) in solid state nuclear track detectors. Experimental procedure and exact material recipes are described; supplies are shown in Table I; a schematic is shown in Fig. 1; a summary of results from all 33 runs

TABLE I. Chemicals and magnets utilized in experiments.

Chemical/ component	Amount/ concentration	Purity/grade	Source (part)
D ₂ O	125 ml	99.8%	alfa.com (14 764-30)
LiCl	150 mM	99.995%	alfa.com (44 762-22)
PdCl ₂	1.25 mM	99.999%	alfa.com (43 085-06)
RhCl ₃	0.00–0.75 mM	99.9%	alfa.com (11 815-03)
Pt wire	0.25 mm dia.	99.997%	alfa.com (10958-CB)
NdFeB magnets	0.27 T	Grade N42	kjmagnetics (BY0Y08)

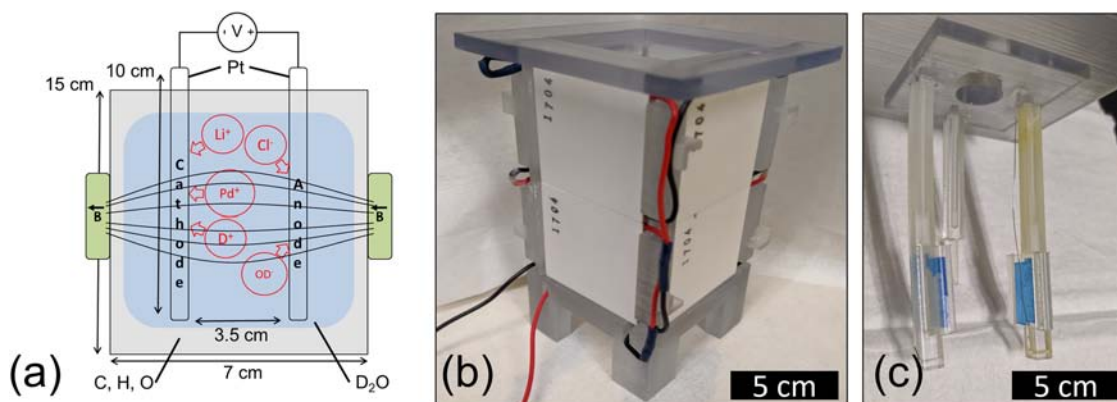


FIG. 1. Experimental protocol and hardware showing: (a) nominal dimensions and elements (not to scale), (b) electrochemical cell body with integrated Seebeck effect sensors connected in series, and (c) electrochemical cell top with thin platinum electrodes being supported by plastic posts and CR-39 solid-state nuclear track detectors arranged inside integrated carriers. All three posts extend into the electrolyte solution and are hollow to allow for three thermocouples to measure cell temperature.

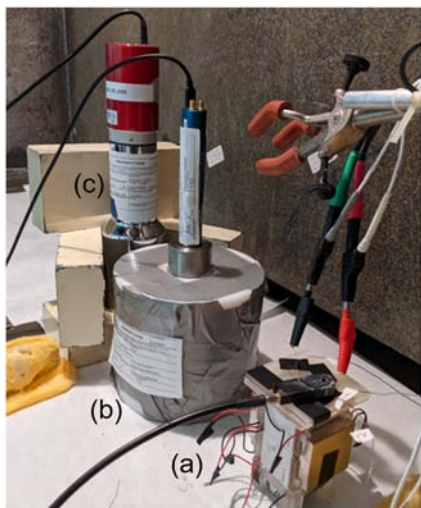


FIG. 2. Image from the NSWC Indian Head Division chemistry laboratory fume hood, showing (a) electrochemical cell utilized in experiments, (b) neutron detector comprising He-3 tube, electronics, and plastic moderating ring encircling tube, and (c) NaI gamma-ray detector, with lead bricks behind it.

is shown in the supplementary material. Some results included in this work were not deemed to be conclusive evidence of unexplained anomalies but are still shown for completeness and transparency.

This work attempted to find evidence of nuclear-origin particles or secondary effects caused by nuclear reactions, which present physical theory state should not occur in electrochemistry experiments run with standard equipment found in academic chemistry laboratories. No particle accelerators, neutron generators, or similar equipment were employed, so if, e.g., output particles with mega electron-volt (MeV) levels of kinetic energy were detected, from chemistry inputs on the order of electron-volts (eV), this would not be expected in traditional electrochemistry environments.

Figure 2 shows electronic neutron and gamma detectors and their proximity to the electrochemical cell hardware. This setup

was modeled utilizing the Monte-Carlo method, as seen in the supplementary material.

Among 33 total experimental runs, 6 runs (and one Li-only control run prior to numerical assignments) had CR-39 results. A greater number of CR-39 analyses could not be completed due to the lack of resources. Table II displays all CR-39 results including the experimental run number; the highest electrolyte temperature seen during run recorded by any of the three thermocouples; total run thermal output energy above and beyond that expected based on input electrical energy and measured via Seebeck effect sensors to 6σ significance; RF signals recorded by current probe clamped onto cathode wire; the highest density of tracks (0.1–20 MeV particle damage locations) found on CR-39 solid state nuclear track detectors per millimeter squared area; and whether statistically significant numbers of neutrons were detected by real-time neutron detector, compared to a background count period directly preceding experiment. Not shown on chart were measurements of tritium content in samples examined post-experiment. At least one examined sample was positive for tritium content, but this was determined to be due to tritium content in D_2O ; details are in the supplementary material. Gamma detector was also only brought online during the last two experimental runs (32 and 33), and no unusual gamma activity was detected.

Figure 3 displays representative results from the use and analysis of CR-39 solid-state nuclear track detectors. These are plastic chips, utilized in fields such as health science (neutron dosimetry),¹⁷ detection of cosmic radiation in space,¹⁸ and monitoring of nuclear reactions in inertial confinement fusion experiments.¹⁹ Two separate partner institutions, working independently with no collaboration, etched CR-39 chips from multiple experiments and found evidence of damage from nuclear-energy particles, likely between 0.1 and 20.0 MeV (energy resolution of CR-39^{18,19}).

DC currents and voltages utilized in this effort [approaching 1 amp (A) and 30 volts (V)] are much higher than those utilized in typical electrochemistry experiments, which are often in the milli-amp (mA) and several volt range. Water electrolyzes at 1.2 V, and some commercial battery chemistry operates at roughly 3.7 V, so most research takes place below 10 V. Prior researchers have theorized that anomalous behavior in Pd experiments is positively correlated with electrical current density through the cathode,²⁰ so the present effort is utilizing this relatively underexplored

TABLE II. Summary of experiments with CR-39 results.

Experiment	T_{\max} (°C)	6σ net energy (kJ)	RF freq. (MHz)	CR-39 tracks (mm^{-2})	Real-time neutrons
00: ^a Li-only	64	<0	None	<100	n/a
03: Li + Pd + Rh	66	+75	92, 311	4600	n/a
09: Li + Pd + Rh	68	−175	None	1600	n/a
11: Li + Pd + Rh	62	−140	None	850	n/a
29: Li + Pd	66	−50	20	2500	None
30: Li + Pd	68	−65	21	5000	$2.3\sigma^b$
31: Li + Pd	64	−55	3, 21	2500	$1.9\sigma^b$

^aLi-only control run accomplished early in effort before formal numbering of experiments.

^bNeutron counts included here for completeness but issues with interpretation are addressed in text.

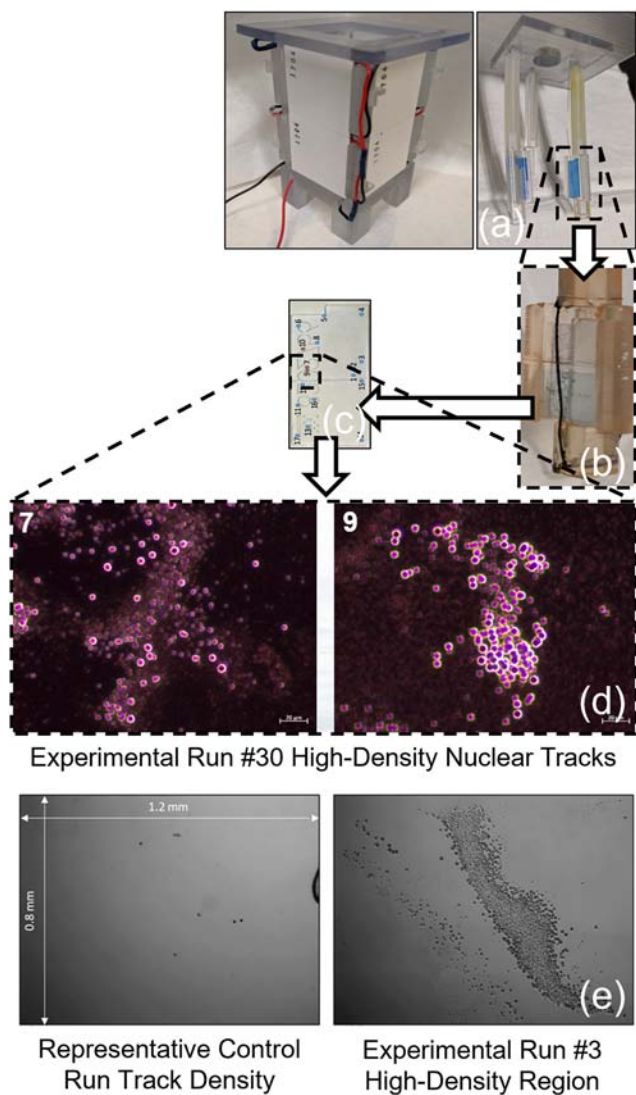


FIG. 3. Representative CR-39 solid-state nuclear track detector results: (a) CR-39 loaded into slots on cathode and anode electrode support posts, before being immersed into electrochemical solution; (b) cathode post tip shown after experiment, discolored from electrochemical bath, with black electroplated metallic layer visible on cathode; (c) same CR-39 chip shown removed from holder, cleaned, etched and ready for optical analysis; (d) optical analysis results of this chip from one collaborating lab, showing high-density tracks indicative of damage caused by nuclear particles with kinetic energy likely between 0.1 and 20.0 MeV; (e) results from two separate experiments, analyzed by a second collaborating lab (independent of collaborator above), showing a lack of tracks in chip from Li-only control run, and regions of high-density tracks in experimental run containing Pd and Rh.

parameter space, in an effort to increase the likelihood of detecting such unusual behavior. Due to this relatively high amount of power put through the electrodes, the electrolyte will heat up to temperatures between 50 and 100 °C. This heat was measured in two ways: thermocouples placed inside the plastic posts descending into

the electrochemical cell measured temperature and Seebeck-effect sensors attached on five sides of the cell (top was open to allow gasses to escape, for safety), measuring thermal flux through the cell walls.

Figure 4 shows two representative experiments, one without Pd metal (a) that does not display anomalous heat flux through Seebeck sensors and one with Pd metal present (b) that does. Total power output through the Seebeck sensors was integrated to calculate total output energy, with $\pm 6\sigma$ error bars (as described in the supplementary material). Total input power from the power supply was also integrated to calculate total input energy, also with $\pm 6\sigma$ error bars. A conservative measure of net experimental energy was calculated by subtracting the total input energy plus 6σ from the total output energy minus 6σ , yielding a positive value when anomalous heat was present to high statistical significance. For electrochemistry experiments with only Li metal and experiments with Rh and/or Pd that did not show heat flux anomalies, this value was always negative, indicating that more energy went into the experiment than was expelled thermally through the walls when conservative error bars were taken into consideration. Without the error bars, net energy in equals net energy out, indicating that the experiment behaved the same way as the Li-only calibration runs. Six experiments with Pd metal added showed positive 6σ net energy in the present effort.

In 1993, researchers at Texas A&M University reported that electrochemical experiments based on Pd metal could be stimulated with RF input at certain key frequencies to produce anomalous heat.²¹ These frequencies were both analytically calculated and later verified experimentally to be roughly 82, 366, and 534 MHz, corresponding to the nuclear magnetic resonance of deuterium, a neutron, and a proton, respectively.²¹ The present work only passively listened for RF and did not attempt to stimulate the experiments with RF. Initial experiments 01–17 listened at the three frequencies specified by the Texas A&M team to determine whether the system was excited in any of these narrow bands, and the results can be seen in Fig. 5. The present work detected anomalous RF signals in the first 17 experiments between 80 and 100 MHz and between 310 and 315 MHz, which were both within 15% of the values predicted and verified by the Texas A&M team. After hardware and software upgrades, subsequent experiments 18–33 listened continuously from low MHz up to low GHz in an attempt to determine whether other frequencies were present, which might have evaded the narrow initial measurement ranges. Results are shown in the supplementary material and include additional anomalies detected between 0.5 and 10 MHz.

After experiments were run inside of Department of Defense facilities, remaining electrolyte with precipitates and electrodes with material deposits were transferred to Department of Commerce and academic partner laboratories for detailed material analysis. A summary of on-wire morphologies can be seen in Fig. 6, and electrodeposited material structure mapping can be seen in Fig. 7. Morphologies were deemed to be consistent with expected electrochemical deposition, and no anomalous elements were detected during compositional analyses. However, the best structural fit was to an unusual material structure, comprising Li_2PdD_4 . This type of structure is normally reported only under high temperature and pressure conditions significantly above those observed in the present work.

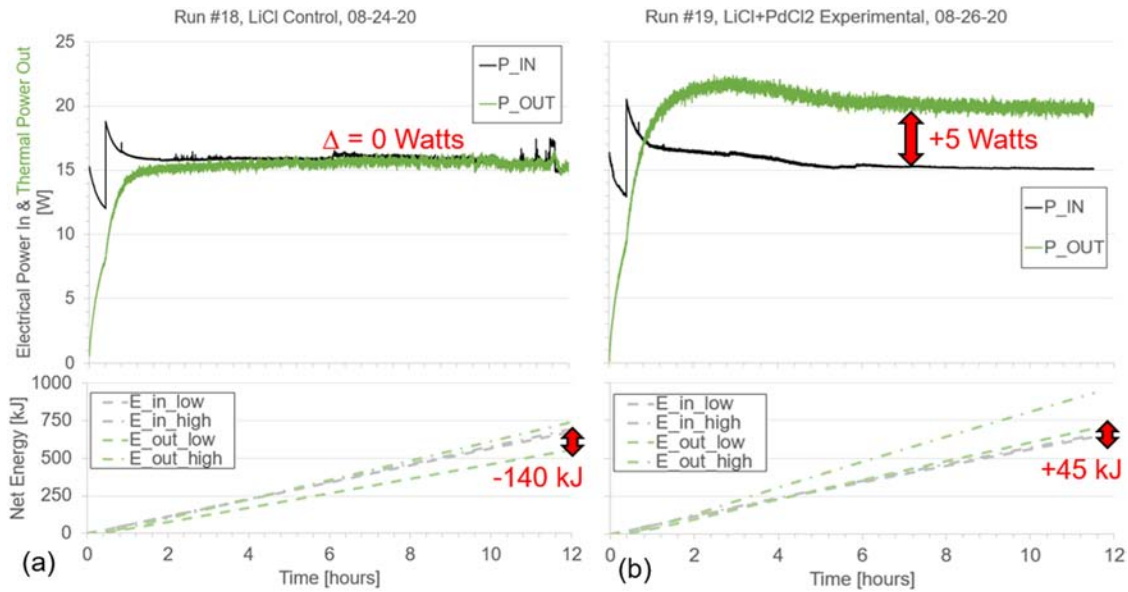


FIG. 4. Comparison of first 12 h of two experiments: (a) Li-only control run and (b) Li + Pd experimental run. These experiments utilized identical hardware, were performed two days apart, and the only difference in the chemical ingredients was the inclusion of PdCl₂ in run (b). Two power measurements are plotted on the left axes: electrical power input from DC power supply to energize the experiment and thermal flux power output from Seebeck sensor surrounding cell. These values are integrated to determine total energy in and energy out, which is plotted on the lower energy plot. At every time step (1 Hz resolution), the previous 30 s and future 30 s are utilized to calculate the moving average at the present time and calculate upper and lower bounds plotted to six sigma significance (6 standard deviations) above and below moving average. Finally, at the end of the run, the most conservative output value ($E_{out-low}$) is subtracted from the most optimistic input value ($E_{in-high}$), and this is reported as the six sigma net energy. If this value is positive, as in run 19, it gives a very conservative indication that there was anomalous heat, above and beyond that expected for the given input electrical power, across the entire experiment. A negative six sigma energy indicates the expected result, where the input and output energies are overlapping, and no unusual thermal events have occurred, to six sigma statistical significance. Dashed and dotted-dashed black lines represent lower and upper bounds on input energy, which is less variable due to the highly accurate power supply utilized, and green lines represent bounds on output thermal energy, which is more variable due to noise inherent in Seebeck sensors.

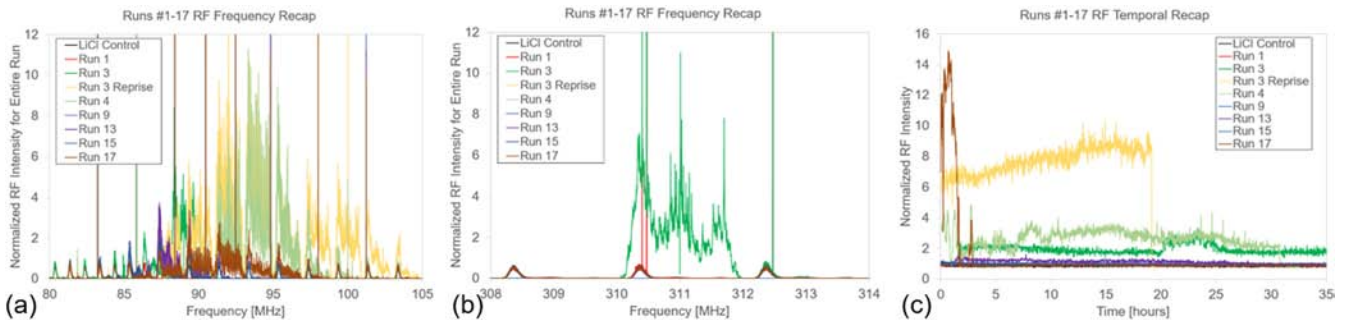


FIG. 5. RF data across first 17 runs. Raw data with no post-processing applied. RTL-SDR hardware (see the supplementary material) was utilized, with y-axis showing intensity (normalized to control runs; larger value equals larger presence of RF). (a) shows the frequency listening range between 80 and 105 MHz, (b) shows results between 308 and 314 MHz, and (c) shows temporal results, indicating RF waveforms appeared at different times during different runs.

Material science results indicate the structure created through the electrode-position may at least partially comprise Li₂PdD₄, and this structure was modeled utilizing the quantum mechanical approach of density functional theory (DFT), with openly available software.¹⁶ Mirroring the experimental conditions seen in the laboratory, this structure was modeled with DC electrical current

flowing through the cell to determine whether under specific conditions, it would be possible for deuteron (D) vibrations to achieve levels of kinetic energy capable of allowing D + D fusion to occur within the unit cell. The molecular dynamics model operates under various assumptions, including in-plane symmetric phonon mode (motion) of D atoms relative to stationary Li and Pd atoms and sin-

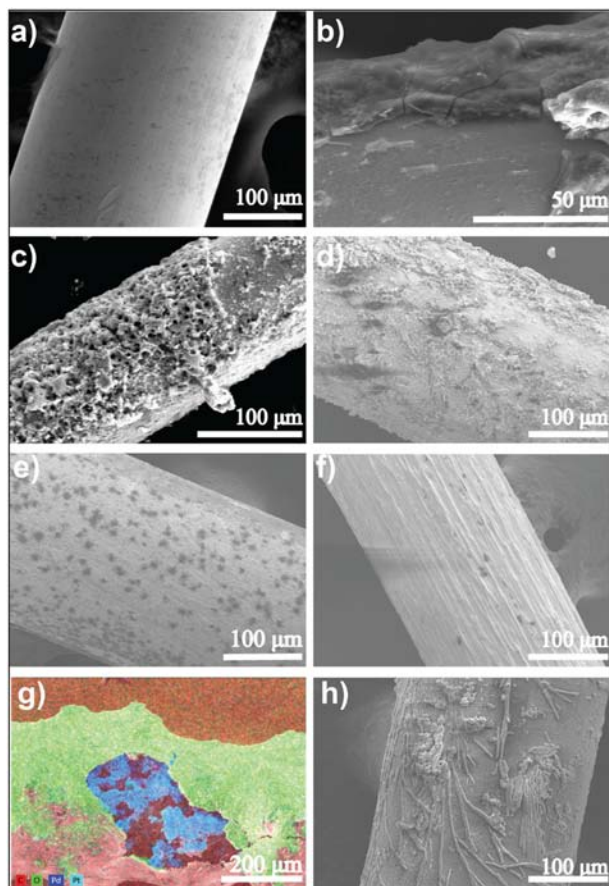


FIG. 6. Visual summary of all types of distinct on-wire morphologies observed through this effort: (a) as-received Pt wire (no processing), (b) non-anomalous run w/Li + Pd + Rh (run 2), (c) anomalous experimental run (run 13) with Li + Pd + Rh, (d) anomalous experimental run (run 17) with Li + Pd + Rh, (e) anomalous Li-only "calibration" experiment (w/some Pd plating due to incomplete cell cleaning) (run 24), (f) anomalous Li + Pd experiment (run 9) after aqua regia digestion, (g) EDX mapping of anomalous Li + Pd experiment (run 32), and (h) non-anomalous calibration Li-only experiment (run 18).

gle electronic charges moving into and out of cell in time (current parametric pumping). The results seen in Fig. 8 show the potential likelihood of atoms reaching kinetic energies required for nuclear reactions inside the metal lattice. Due to uncertainties within the initial material science related to energy loss from first-order allowed electronic transitions, this is a preliminary model only and not claimed to be descriptive of the actual atomic dynamics at work in the present experiments.

Possible non-nuclear explanations for all reported anomalous results, along with final determinations by the project team, are discussed. A number of experimental recipes were undertaken, varying materials, electricity (electric field), and magnetic field directions (relative to one another), and the most repeatable recipes are detailed, which could be utilized by other teams in replication efforts.

The present effort considered the following possible prosaic explanations for the reported nuclear anomalies:

- CR-39 damage due to heat from electrodes/electrolyte.
- CR-39 damage due to electric-field driven chemical ion ablation (mechanical damage).
- Neutron/gamma spikes due to cosmogenic/background sources.

Other researchers previously discussed similar questions regarding possible alternate explanations for tracks while utilizing the 2013 procedure.^{8,22} In the previous reporting, tracks were not uniformly seen across all CR-39 chips utilized in experiments under identical experimental conditions, and they concluded that chemical attack was not the source of their observed tracks. Analogously, in the present work, CR-39 chips were utilized at both anode and cathode locations, which experienced almost identical chemical-thermal profiles during electrolysis. Tracks were not observed equally at both electrodes but were concentrated at locations adjacent to cathodes, where the metal plating reaction occurs. This plated layer on the cathode is the location of putative nuclear particle generation. The absolute number of CR-39 measurements in the present effort was low due to resource constraints, but the initial results obtained here mirror prior results in this area. Further study, including detailed analysis of CR-39 chips from both anode and cathode experiments across a large number of experiments, should be undertaken in the future. Overall, 100% of analyzed CR-39 chips supported the hypothesis that nuclear particles were generated at the experimental cathodes. Additionally, multiple conversations with the U.S. government and private labs who have utilized CR-39 have not produced any mechanisms by which track-like damage could occur through localized heating or mechanical damage.

CR-39 track dimensions were computed, and statistical analysis found their diameters between 6.11 ± 1.52 and 9.19 ± 1.14 μm , which was consistent with other reporting,⁸ and similar to our own results when exposing virgin CR-39 chips to a Thorium-230 alpha-particle emitter (see Fig. 9), which were between 3.82 ± 0.39 and 6.13 ± 1.38 μm .

A He-3 based real-time neutron detector was integrated into seven experiments, and a NaI based real-time gamma ray detector was integrated into two experiments. Over the course of the final seven experiments, four experiments appeared to have higher average neutron counts during experiments, compared to the non-experimental background counts immediately preceding them. However, when examining background counts against one another over the course of two months, significant variation was seen, and no other real-time neutron data inside the same laboratory were available for comparison.

Efforts were made to find external background data from other laboratories, and this is detailed in the supplementary material. However, overall our team found these data not conclusive of neutron activity above background. These experiments should be repeated with multiple identical detectors running simultaneously, both adjacent to electrochemical cells and a statistically significant distance away inside the same laboratory.

Data collected using a 3×3 in. sodium iodide based gamma ray detector over several runs did not find anomalous gamma isotopic energy lines as compared with background. Overall gamma

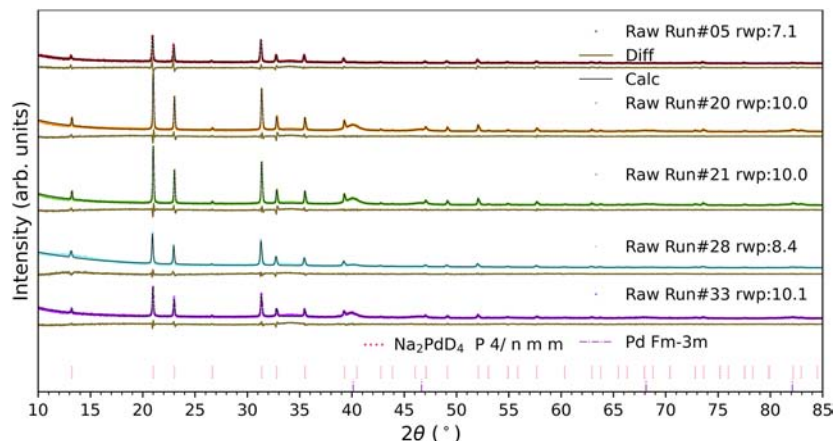


FIG. 7. XRD diffraction comparison of run 5 (Li + Pd + Rh), 20 (Li + Pd), 21 (Li + Pd), and 33 (Li + Pd). Run 33 was electrolyzed for roughly 40 h, compared to roughly 12 h for the other experiments. This analysis suggests that the electroplated structure may comprise Li_2PdD_4 , which is unusual due to being analogous to structures typically generated at extremely high pressure and temperature, such as Na_2PdH_4 , but further study is necessary to confirm.

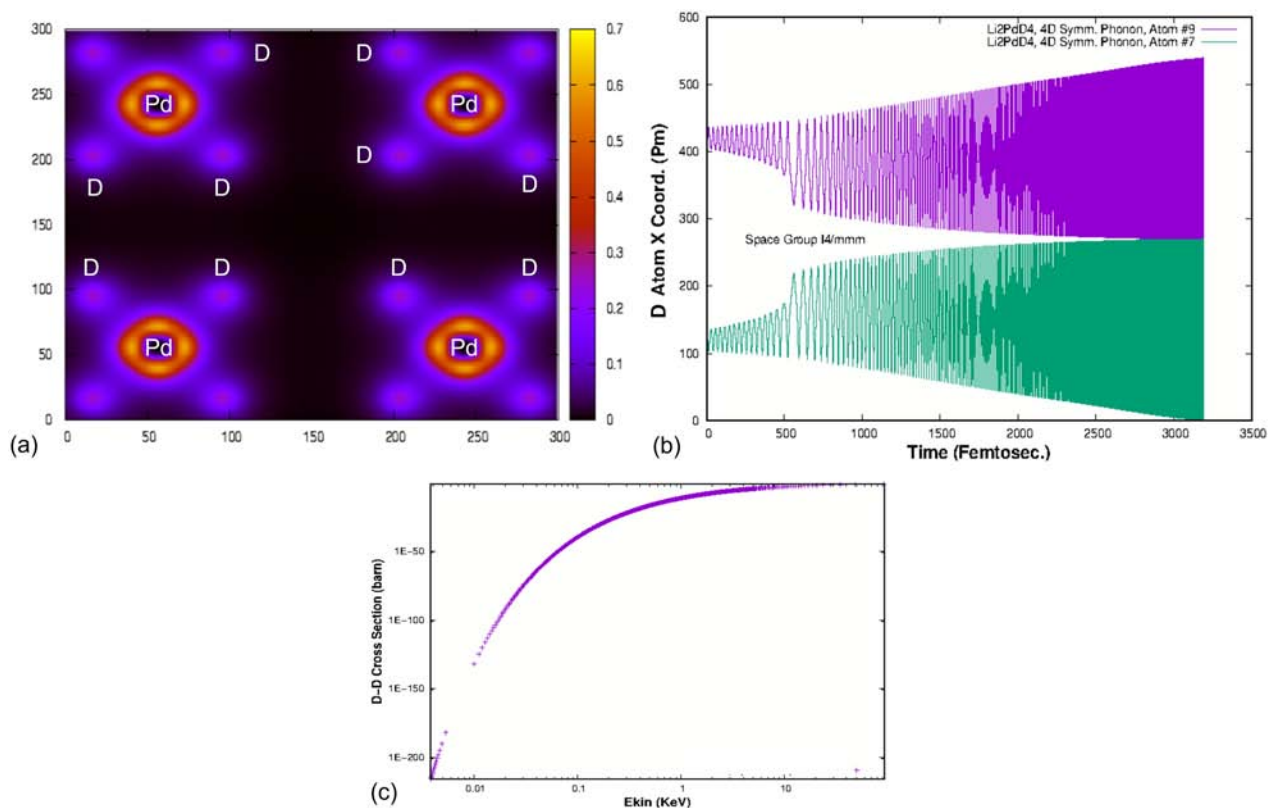


FIG. 8. (a) Structure of the Li_2PdD_4 modeled system, showing atoms in a single plane containing Pd and D (Li atoms exist on parallel plane). (b) Molecular dynamics of D atoms in assumed symmetric phonon mode; Li and Pd atoms are much larger than D, and D atoms move orders of magnitude more during electronic charge pumping, so only they are dynamically modeled. This chart shows vibrations increasing in amplitude and hardening over time. (c) Calculations of D + D fusion cross section in barns, based on kinetic energies of D atoms during electronic pumping, show increasing probability of fusion, reaching 1 b in less than 4 ps, indicating that D + D fusion would be likely under the assumptions of this model.

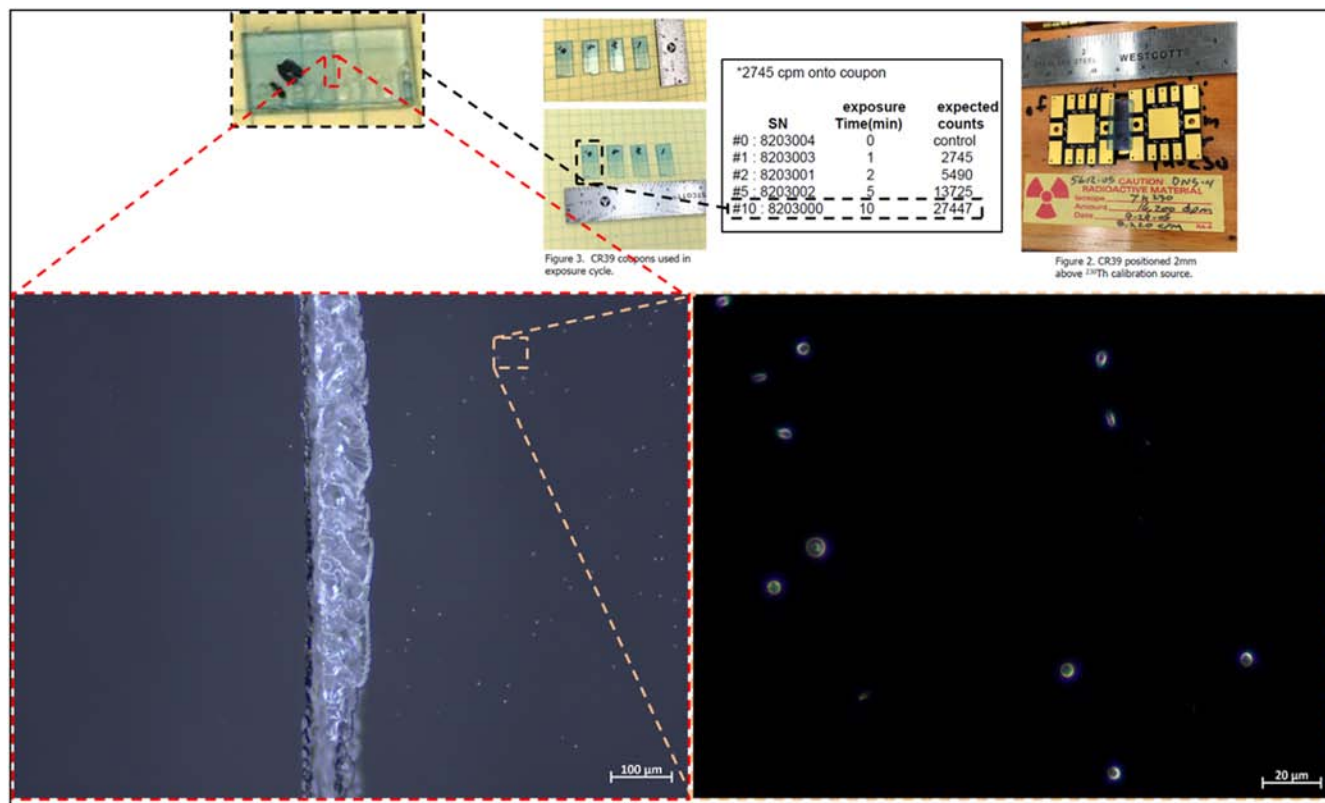


FIG. 9. Virgin chip exposure to the Th-230 4.7 MeV alpha source. Half of each chip was covered with polyethylene protective coating, and the etched image on left shows less tracks on the left-hand side (covered) and relatively more on the right-hand side, showing coating acted as a filter for 4.7 MeV alphas. This same approach of removing half of the protective barrier was carried out during experimental runs to help discriminate tracks based on energy and rule out chip-wide non-nuclear anomalies.

energy count rates over the collected spectrum did not show elevated counts on average. Future runs would benefit from shielding to minimize background noise and to allow for the easier identification of anomalous gamma energy lines. Additional detectors, and detectors with improved resolution, such as high purity germanium, may also prove beneficial in future research by allowing better identification of relevant gamma energy lines. Detectors that could be positioned closer to the test cell, or inside the test cell, would also be beneficial. Multiple redundant detectors should also be utilized in future efforts.

The present effort also considered the following possible prosaic explanations for the reported 6σ net energy anomalies:

- Chemical reactions inside the electrolyte, between the water and salts in each experimental run.
- Recombination of hydrogen and oxygen gasses liberated during electrolysis.
- Joule heating due to relatively high levels of current through electrodes.
- Inaccuracies inherent in thermal measurement systems.

Building a full mechanistic model of the chemistry involved in these experiments would have entailed a large sub-effort, out of the scope

of the present work. However, the chemists and material scientists on our team do not expect that such an analysis would reveal a reaction capable of producing the heat levels recorded. If the electrochemical cells were completely closed, with no possibility of gas escape, hydrogen–oxygen recombination and gas pressure explosions would be a concern. For these reasons, the cell is open on top, and experiments were completed in a fume hood to minimize these safety concerns. Joule heating of the electrodes will create heat due to the relatively large current densities utilized in this effort; however, this effect should be constant across experiments. Wire diameter, orientation, and max current levels were not changed across the majority of experiments. Therefore, if two experiments have comparatively different levels of anomalous heat with the same electrical inputs, the chances that this is attributable to Joule heating are low. There could have been inaccuracies in our thermal measurement system, including small variations in Seebeck sensors across experimental cells. However, the Seebeck sensors were calibrated when introduced, and all thermal results were consistently recorded across tens of experiments, lessening the chances of thermal measurement inaccuracies leading to the anomalous heat results reported.

The present effort also considered the following possible prosaic explanations for the reported RF anomalies:

- Outside radio/cellular signals being picked up in the laboratory.

DARPA facilitated conversations between this project team and outside experts in environmental electromagnetic noise to discuss possibilities for outside interference causing the signals observed. All parties were in agreement that signals at frequencies higher than roughly 650 MHz could potentially be due to cellular and/or portable radio traffic, but there were no general concerns for lower-frequency anomalies. Our effort contacted other organizations across both Dahlgren and Indian Head naval bases that may be engaging in electromagnetic testing to cross-reference days and frequencies, looking for signals in the present experiments that may have come from other sources. No outside sources of signal interference <650 MHz were identified to have caused the results shown here, and the possibility is open that signals detected above 650 MHz were the result of nearby cellular traffic.

Finally, material analysis did not detect any strong evidence for nuclear-origin effects, including transmutation of elements. Electrodeposited structure appears to be consistent with typical electrochemical results, despite the higher magnitude input electrical power. The most compelling result from these analyses was the initial determination of an unusual material structure present in the electroplated material, comprising Li_2PdD_4 . This type of structure is normally synthesized at high temperatures and pressures, significantly above standard conditions, and the present procedure may be a new low-pressure, low-temperature synthesis route for similar materials. More analysis is needed on this topic, and a separate paper will be published in the future delving into more detail.

Across the 33 numbered experiments reported here, various recipes were investigated based on combinations of the following variables:

- Inclusion of Rh metal and its ratio compared to Pd.
- Maximum value of electrical current.
- Relative orientation of electric field between the cathode and anode, and static magnetic field supplied by bar magnets on sides of the electrochemical cell.

Table III compiles all experiments attempted with Li + Pd metal (no Rh), a step increase in current from 700 mA (initial) to 900 mA (after electrolyte has warmed up for 25 min), and parallel magnetic and electric fields. This combination produced the largest amount of total positive CR-39 data, indicating the presence of nuclear activity. It is not known to what extent the field orientation affected these

TABLE III. Results from recipe with most repeatable nuclear results: Li + Pd; 0.7, 0.9 A; perpendicular electric and magnetic fields.

Experiment	RF (MHz)	CR-39 tracks (mm ⁻²)	Neutrons	6 σ net energy (kJ)
29, Li + Pd	20	2500	None	-50
30, Li + Pd	21	5000	2.3 σ^a	-65
31, Li + Pd	3, 21	2500	1.9 σ^a	-55

^aNeutron counts included here for completeness, but issues with interpretation are addressed in text.

three experiments, compared to others with parallel fields. Previous work with the same patented procedure reported effects of magnetic fields on experiments with observed tracks in CR-39.²²

In Fig. 1, a schematic of the electrochemical experiment is shown in panel (a), not to scale. The gray rectangle represents the rapid prototyped plastic electrochemical cell body [seen in (b)], with the blue rectangle representing D_2O poured inside it. The red circles represent the chloride salts that have been placed into solution and dissolved into their constituent ions, and the green rectangles represent rare earth magnets.

When the electrodes are energized with a DC electrical current, an electron surplus at the cathode reduces the valence state of positively charged ions (cations) in its vicinity. Lithium (Li^+), deuterium (D^+), palladium (Pd^{+2} , if present), and rhodium (Rh^{+3} , if present) cations are electrostatically attracted to the cathode, forming a surface plated metallic alloy film on the cathode that is loaded with deuterium immediately upon formation. This is the location of potential non-chemical reactions being investigated. Deuterium ions that do not enter the plated film are reduced at the cathode to form neutral deuterium gas bubbles that then separate from the cathode, rise to the surface of the electrolyte, and escape from the cell via the hole in the cell lid. The electron deficiency at the anode oxidizes the negatively charged ions (anions), such as chlorine (Cl^-) and deuterioxide (OD^-) or oxygen (O^{-2}), that are electrostatically attracted to the anode by its positive potential. These form bubbles at the anode and are released as free molecules of Cl_2 and O_2 gas. Since Cl_2 is toxic to humans and the mixture of O_2 and D_2 gases is known to be highly combustible, the experiment must be conducted in a well-ventilated fume hood for personnel safety. Future efforts could design and execute experiments with completely closed electrochemical systems, utilizing recombining elements to prevent gas explosion, but this was out of scope of the present work. Figure 1(b) shows the rapid prototyped cell body, composed of the elements carbon (C), hydrogen (H) and oxygen, and Fig. 1(c) shows the rapid prototyped cell top (same material).

The cell bodies are surrounded on all sides, except the top, by a series of square solid-state thermoelectric devices operated in passive mode (no current being forced) as Seebeck sensors. These are connected in series, so that their individual voltage outputs are summed to form an overall output voltage that can vary from 0 to roughly 1 V and will be linearly proportional to the thermal flux passing across the boundary of the cell. The calibration procedure and data can be seen in the supplementary material. The cell top has three posts extending down into the electrolyte mixture, all of which are hollow to allow for thin thermocouple wires to record temperature inside the cell, without coming into physical contact with the electrolyte. Two posts also serve to physically support the thin platinum (Pt) cathode and anode wires, which conduct electricity into the cell and on the cathode side provide a substrate for the Pd alloy electrodeposited layer(s). Also visible in Fig. 1(c) are the CR-39 solid-state nuclear track detectors (blue), which are held in place adjacent to both cathode and anode wires. A static magnetic field (B-Field) is provided by two NdFeB bar magnets with a strength of 2704 G (0.27 T). Visible in Fig. 2 is the current probe, attached to a long black semi-rigid coaxial cable, which clamps around the cathode wire outside the cell, to monitor for radio frequency emissions through the cathode during experiments.

In conclusion, this effort reports anomalous thermal, RF, and nuclear-origin results, correlated across multiple experiments, which our team believes is initial evidence of nuclear activity in the studied electrochemical systems, based on the 2013 Navy procedure. Result datasets comprise CR-39 solid-state nuclear track detector damage potentially caused by 0.1–20 MeV particles; watts of thermal flux from cells, above and beyond that expected based on electrical inputs; and RF signals multiple dB above the noise floor that began during electrochemical runs. The most successful experimental recipe, comprising heavy water, lithium, and palladium chloride salts, showed positive CR-39 data across 100% of experiments (3/3 trials), indicating that this procedure is repeatable and will allow for future replication by other groups. Thermodynamic and structural analyses confirm that material generated during the effort consists of Pd alloys with a high degree of deuterium loading, which is one of the primary assumptions of our theoretical DFT model. Furthermore, material analysis revealed the formation of at least two Pd compounds: a novel Li_2PdD_4 palladate phase, normally synthesized under high pressure, and a nano-sized Pd metal, both of which should be studied in greater detail in the future work. DFT modeling indicates that electrical pumping of the type supplied in these experiments could cause deuterium molecules to reach kinetic energies inside the lattice capable of initiating nuclear reactions, indicating that this phenomenon may be reasonably assumed to occur, within the assumptions of this model.

The totality of this work indicates initial, but not overwhelming, evidence of nuclear reactions initiated through electrochemical experiments, reproducible in a standard chemistry laboratory. In order to potentially gather the overwhelming evidence necessary for the scientific community to conclude that this is a new physical phenomenon, a greater diversity of nuclear detection schemes would be needed. This should include the use of redundant detectors measuring background levels concurrently and potentially new hardware design to allow detectors to be placed within the electrolyte in close proximity to the electroplated area on the cathode (which is the most likely location of nuclear reactions).

The supplementary material contains additional data supporting the conclusions of this paper and is included for completeness.

The authors would like to thank Efrain E. Rodriguez from the University of Maryland for his helpful discussions regarding characterization of the Pt electrodes and material analysis and Marcus J. Carter of the National Institute of Standards and Technology, Center for Neutron Research, for assistance with material characterization. The authors would also like to acknowledge the financial support and leadership provided by Michael Fiddy and Lt. Col. David Lewis of the DARPA Defense Sciences Office. This work would not have been possible without their efforts. This research was developed with funding from the Defense Advanced Research Projects Agency (DARPA). The views, opinions, and/or findings expressed are those of the authors and should not be construed to represent the official views or policies of the Department of Defense or the U.S. Government (Contract No. HR0011045611).

AUTHOR DECLARATIONS

Conflict of Interest

The authors have no conflicts to disclose.

Author Contributions

Carl Gotzmer: Conceptualization (equal); Funding acquisition (equal); Investigation (equal); Project administration (equal). **Louis F. DeChiaro:** Conceptualization (equal); Data curation (equal); Formal analysis (lead); Validation (equal); Writing – original draft (equal). **Kenneth Conley:** Funding acquisition (equal); Project administration (equal); Resources (equal); Supervision (equal). **Marc Litz:** Formal analysis (equal); Investigation (equal). **Marshall Millett:** Formal analysis (equal). **Jesse Ewing:** Formal analysis (equal). **Lawrence P. Forsley:** Formal analysis (equal). **Karen J. Long:** Formal analysis (equal); Investigation (equal). **William A. Wichart:** Investigation (equal). **Pamela A. Mosier-Boss:** Formal analysis (equal). **John Sullivan:** Formal analysis (equal); Investigation (equal); Software (equal). **Efrem Perry, Jr.:** Investigation (equal). **Oliver M. Barham:** Conceptualization (equal); Data curation (lead); Formal analysis (equal); Funding acquisition (lead); Investigation (lead); Methodology (lead); Project administration (lead); Resources (lead); Supervision (lead); Writing – original draft (lead); Writing – review & editing (lead).

DATA AVAILABILITY

The data that support the findings of this study are available within the article and its supplementary material.

REFERENCES

- ¹M. Fleischmann and S. Pons, “Electrochemically induced nuclear fusion of deuterium,” *J. Electroanal. Chem. Interfacial Electrochem.* **261**(2), 301–308 (1989).
- ²*Cold Fusion Research*, edited by J. W. Landis (U.S. Department of Energy, Washington, DC, 1989).
- ³S. E. Jones *et al.*, “Observation of cold nuclear fusion in condensed matter,” *Nature* **338**(6218), 737–740 (1989).
- ⁴S. Szpak *et al.*, “On the behavior of Pd deposited in the presence of evolving deuterium,” *J. Electroanal. Chem. Interfacial Electrochem.* **302**(1–2), 255–260 (1991).
- ⁵S. Szpak *et al.*, “Absorption of deuterium in palladium rods: Model vs. experiment,” *J. Electroanal. Chem.* **365**(1–2), 275–281 (1994).
- ⁶S. Szpak *et al.*, “On the behavior of the cathodically polarized PdD system: Search for emanating radiation,” *Phys. Lett. A* **210**(6), 382–390 (1996).
- ⁷S. Szpak *et al.*, “Further evidence of nuclear reactions in the Pd/D lattice: Emission of charged particles,” *Naturwissenschaften* **94**, 515 (2007).
- ⁸P. A. Mosier-Boss *et al.*, “Use of CR-39 in Pd/D co-deposition experiments,” *Eur. Phys. J. Appl. Phys.* **40**, 293–303 (2007).
- ⁹P. A. Mosier-Boss *et al.*, “Triple tracks in CR-39 as the result of Pd-D co-deposition: Evidence of energetic neutrons,” *Naturwissenschaften* **96**, 135–142 (2009).
- ¹⁰P. A. Mosier-Boss *et al.*, “Comparison of Pd/D co-deposition and DT neutron generated triple tracks observed in CR-39 detectors,” *Eur. Phys. J. Appl. Phys.* **51**, 20901 (2010).
- ¹¹P. J. Smith *et al.*, “Electrolytic co-deposition neutron production measured by bubble detectors,” *J. Electroanal. Chem.* **882**, 115024 (2021).
- ¹²C. P. Berlinguette *et al.*, “Revisiting the cold case of cold fusion,” *Nature* **570**, 45–51 (2019).

- ¹³U. Szczecinski, Clean Energy from Hydrogen-Metal Systems, Grant Agreement ID: 951974, Overall budget €5,678,597 (2020).
- ¹⁴T. Yliopisto, Breakthrough zero-emissions heat generation with hydrogen-metal systems, Grant agreement ID: 952184 Overall budget €3,999,870 (2020).
- ¹⁵Navy, "System and method for generating particles," U.S. Patent 8,419,919B1 (04/16/2013).
- ¹⁶P. Giannozzi *et al.*, "QUANTUM ESPRESSO: A modular and open-source software project for quantum simulations of materials," *J. Phys.: Condens. Matter* **21**(39), 395502 (2009).
- ¹⁷G. W. Phillips *et al.*, "Neutron spectrometry using CR-39 track etch detectors," *Radiat. Prot. Dosim.* **120**(1–4), 457–460 (2006).
- ¹⁸J. Palfalvi *et al.*, "Evaluation of solid state nuclear track detector stacks exposed on the international space station," *Radiat. Prot. Dosim.* **110**(1–4), 393–397 (2004).
- ¹⁹F. H. Séguin *et al.*, "Spectrometry of charged particles from inertial-confinement-fusion plasmas," *Rev. Sci. Instrum.* **74**, 975 (2003).
- ²⁰M. C. H. McKubre, "Cold fusion: Comments on the state of scientific proof," *Curr. Sci.* **108**(4), 495–498 (2015).
- ²¹J. Bockris *et al.*, "Triggering of heat and sub-surface changes in PdD systems," Paper presented at the 4th International Conference on Cold Fusion, Lahaina, Maui, 6–9 December 1993.
- ²²P. A. Boss *et al.*, "Condensed matter nuclear reaction products observed in Pd/D co-deposition experiments," *Curr. Sci.* **108**(4), 656–659 (2015).